Carbon Dioxide Fixation | Hot Paper

DOI: 10.1002/ange.201411170

Visible-Light-Driven CO_2 Reduction with Carbon Nitride: Enhancing the Activity of Ruthenium Catalysts**

*Ryo Kuriki, Keita Sekizawa, Osamu Ishitani, and Kazuhiko Maeda**

Abstract: *A heterogeneous photocatalyst system that consists of a ruthenium complex and carbon nitride (C_3N_4), which act as the catalytic and light-harvesting units, respectively, was developed for the reduction of CO_2 into formic acid. Promoting the injection of electrons from C_3N_4 into the ruthenium unit as well as strengthening the electronic interactions between the two units enhanced its activity. The use of a suitable solvent further improved the performance, resulting in a turnover number of greater than 1000 and an apparent quantum yield of 5.7% at 400 nm. These are the best values that have been reported for heterogeneous photocatalysts for CO_2 reduction under visible-light irradiation to date.*

The production of transportable fuels through artificial photosynthesis on a large scale is of interest owing to the increasing demand for renewable energy as an alternative to fossil fuels and nuclear energy.[1] The photocatalytic reduction of CO_2 into energy-rich chemicals has the potential to produce renewable energy while also reducing the amount of the greenhouse gas CO_2.[2–16] One of the two-electron reduction products of CO_2, formic acid, is a useful liquid fuel that can be readily decomposed into H_2 and CO_2 in the presence of a suitable catalyst.[17] Finally, the combustion of H_2 produces a high energy density ($\Delta G° = 238\ kJ\,mol^{-1}$), giving water as the sole product. The reduction/re-oxidation thus completes a carbon-neutral cycle without the release of harmful byproducts.

The seminal work by Lehn et al. in 1983[2] was followed by the preparation of several types of homogeneous (photo)catalysts that are based on metal complexes that contain Re or Ru, which enabled the selective formation of CO or HCOOH.[3–6] In particular, supramolecular complexes with a light-harvesting and a catalytic unit with two or more metal centers possessed improved properties.[6] The number of reports on CO_2 reduction using a heterogeneous photocatalyst under visible-light irradiation has been increasing.[11–16] However, none of these have yielded a satisfactory result; state-of-the-art catalysts enable reactions with turnover numbers (TONs) of approximately 200 and apparent quantum yields (AQYs) of approximately 2%.[11,13a] The present study describes the synthesis of a high-performance heterogeneous photocatalyst for the reduction of CO_2 into formic acid under visible-light irradiation using carbon nitride (C_3N_4) and a Ru complex. By careful design of the catalytically active site and the reaction environment to maximize the efficiency of the CO_2 reduction process, a substantial improvement in photocatalytic performance was achieved, leading to the highest TON (>1000) and AQY (5.7% at 400 nm) reported for such catalysts to date.

Carbon nitride (C_3N_4) is a widely studied functional material for various applications, including heterogeneous (photo)catalysis.[18] C_3N_4 has been used for photocatalytic reactions, including water reduction/oxidation,[19] the decomposition of harmful pollutants,[20] organic transformation,[21] and the production of hydrogen peroxide,[22] and it has also been explored as a photocatalyst for the reduction of CO_2 into formic acid under visible-light irradiation when modified with a molecular Ru^{II} complex (RuCP in Scheme 1).[13] Although C_3N_4 consists entirely of carbon and nitrogen atoms, the formic acid produced originates not from C_3N_4 decomposition, but from photocatalytic CO_2 reduction, as confirmed by isotope tracer experiments with $^{13}CO_2$. In contrast to conventional heterogeneous catalysts for CO_2 conversion, which require high temperatures and pressures,[23] this photocatalytic system works at room temperature and under ambient pressure. This was the first example of reproducible CO_2 reduction using carbon nitride as a visible-light-responsive photocatalyst. Follow-up studies on this hybrid material elucidated the effect of the pore–wall structure of carbon nitride on the photocatalytic CO_2 reduction.[13b] However, no principles for improving the activity of this system were discovered that enable the optimization of the structure of the immobilized metal complex despite its vital role in CO_2 reduction. As a result, the current performance of this system is not satisfactory.

As illustrated in Scheme 1, the immobilized metal complex plays two important roles: It accepts electrons from the conduction band of C_3N_4 and hosts the active site for CO_2 reduction. This suggests that the photocatalytic activity for CO_2 reduction is strongly dependent on the structure of the metal complex employed. Metal complexes can be designed

[*] R. Kuriki, Dr. K. Sekizawa,[+] Prof. Dr. O. Ishitani, Prof. Dr. K. Maeda
Department of Chemistry
Graduate School of Science and Engineering
Tokyo Institute of Technology
2-12-1-NE-2 Ookayama, Meguro-ku, Tokyo 152-8550 (Japan)
E-mail: maedak@chem.titech.ac.jp

[+] Present address: Toyota Central Research & Development Laboratories, Inc.
41-1, Yokomichi, Nagakute, Aichi 480-1192 (Japan)

[**] K. M. acknowledges start-up funding from the Faculty of Science, Tokyo Institute of Technology and a Grant-in-Aid for Scientific Research on Innovative Areas (25107512). We are also thankful to PRESTO/JST for support through the program "Chemical Conversion of Light Energy" and for a Grant-in-Aid for Young Scientists (A) (25709078). This work was partially supported by the Photon and Quantum Basic Research Coordinated Development Program (MEXT, Japan).

Supporting information for this article is available on the WWW under http://dx.doi.org/10.1002/anie.201411170.

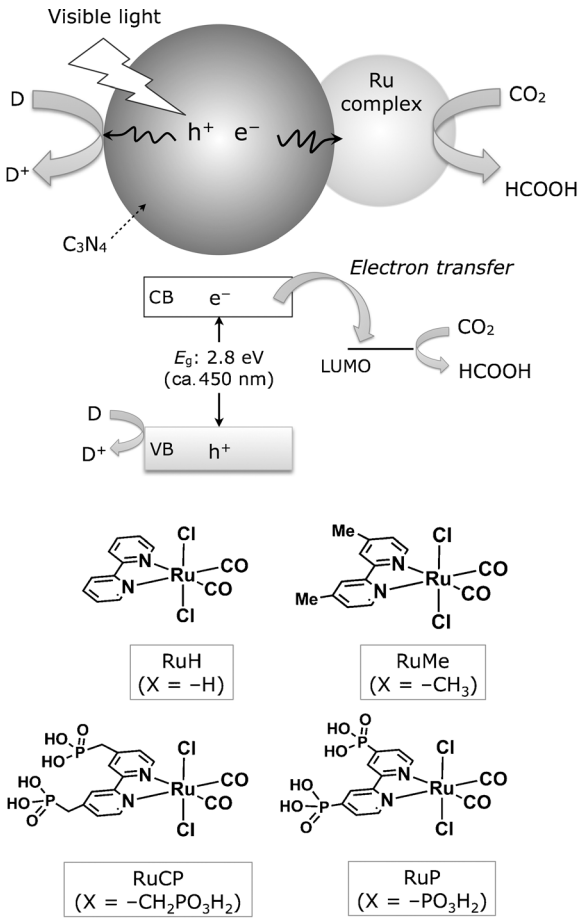

Scheme 1. CO_2 reduction using a Ru complex/C_3N_4 hybrid photocatalyst, along with structures of the Ru complexes used. CB = conduction band, VB = valence band.

on a molecular scale, allowing for an adjustment of the catalytic functionality.[4–6] Guidelines for the preparation of a highly efficient photocatalytic CO_2 reduction system using rhenium(I) complexes in a homogeneous environment have been established by Ishitani et al.[5] Herein, four different Ru complexes, *trans*(Cl)-[Ru(bpyX_2)$(CO)_2Cl_2$] (bpyX_2 = 2,2′-bipyridine with substituents X in the 4-positions, X = H, CH_3, PO_3H_2, or $CH_2PO_3H_2$), were used as kinetic promoters for CO_2 reduction, along with a suitable reaction environment to increase the efficiency of the overall process. The structures of these complexes are shown in Scheme 1, along with their abbreviations.

Graphitic C_3N_4 with 12 nm mesopores (specific surface area: 180 $m^2 g^{-1}$; pore volume: 0.7 $cm^3 g^{-1}$) was used as the building block (represented by C_3N_4 for simplicity). A detailed method for the preparation of such C_3N_4 samples has been reported previously.[13] Functionalization of C_3N_4 with a Ru complex was performed by dispersing the C_3N_4 powder in a methanol solution containing the appropriate amount of a Ru complex with continuous stirring at room temperature overnight. Results indicated that RuP and RuCP were adsorbed quantitatively up to approximately 40 μmol g^{-1}. However, no adsorption was found to occur for RuH and RuMe, which do not have an anchoring group.

To assess the electronic interactions between C_3N_4 and immobilized Ru (RuP and RuCP), FT-IR spectra were recorded. As shown in the Supporting Information, Figure S1, two peaks that can be assigned to the vibration modes of two carbonyl groups, were observed in both cases. It should be noted that carbon nitride alone does not produce any IR bands in this region.[13] The positions of these peaks did not change for the RuCP sample after loading onto C_3N_4, indicating that electronic interactions between C_3N_4 and RuCP and any structural changes in the complex were negligible. This result is reasonable because the $-CH_2-$ spacers between the phosphoric acid groups and the bpy moiety prevent electronic conjugation. In contrast, the positions of the CO ligand peaks of RuP changed when the complex was grafted onto C_3N_4, which suggests that there is an electronic interaction between the loaded RuP and C_3N_4, presumably because of the lack of $-CH_2-$ spacers.

The catalytic activity of the Ru complexes in CO_2 reduction was investigated using an electrochemical technique. Cyclic voltammograms of the Ru complexes in a DMA (*N*,*N*-dimethylacetamide)/TEOA (triethanolamine) mixture containing Et_4NBF_4 (0.1 M) as a supporting electrolyte are shown in Figure S2. Onset potentials for the first irreversible wave, which was attributed to reduction of the diimine (bpyX_2) ligand, ranged from approximately −1.4 to −1.5 V. Under a CO_2 atmosphere, a clear catalytic current that was due to CO_2 reduction was generated at a more negative potential, indicating that all of the Ru complexes tested had the ability to reduce CO_2. However, the onset potentials of the first reduction wave for RuP and RuH were observed at approximately −1.4 V, a potential that is 0.1 V more positive than those of RuCP and RuMe, meaning that RuP and RuH were more susceptible to reduction than RuCP and RuMe. This is reasonable considering that two $-CH_2-PO_3H_2$ (or $-CH_3$) groups lead to an increase in the energy of the π^* orbitals of these complexes because of their electron-donating nature.

Using the prepared hybrid photocatalysts, CO_2 reduction reactions were conducted under visible-light irradiation in MeCN/TEOA (4:1, v/v) saturated with atmospheric CO_2 ($\lambda > 400$ nm). Similarly, reactions were performed using C_3N_4 in a MeCN/TEOA solution with dissolved RuH or RuMe. As shown in Figure S3, C_3N_4 has a steep absorption edge near 450 nm and a tail extending to 600 nm. In contrast, the Ru complexes show little absorption in the visible-light region. Therefore, under visible-light irradiation ($\lambda > 400$ nm), the C_3N_4 component can be selectively activated.

Table 1 lists the activity of C_3N_4 in combination with four different Ru complexes for HCOOH generation under visible-light irradiation ($\lambda > 400$ nm). All of the materials tested, except for RuMe+C_3N_4 (entry 2), were active catalysts of this reaction, but their performance depended on the Ru complex used. The order of activity was: RuP > RuCP ≈ RuH ≫ RuMe. In all cases except for the RuMe-catalyzed reaction, HCOOH was produced in a catalytic cycle as the TONs were greater than one. During the reaction, not only HCOOH, but also small amounts of H_2 and CO were generated. The selectivity of HCOOH production was greater than 80% in all cases.

Table 1: Results of the CO_2 reduction reaction ($\lambda > 400$ nm).[a]

Entry	Photocatalyst	Solvent	Amount of HCOOH formed [μmol]	TON[b]
1	$RuH + C_3N_4$	MeCN	0.8	13
2	$RuMe + C_3N_4$	MeCN	n.d.	–
3	$RuCP/C_3N_4$	MeCN	1.2	20
4	RuP/C_3N_4	MeCN	3.4	55
5	RuP/C_3N_4	DMA	8.8	141
6	RuP/C_3N_4	MeOH	1.2	20
7	RuP/C_3N_4	H_2O	n.d.	–

[a] Reaction conditions: Ru complex (7.8 μmol per gram of C_3N_4)/C_3N_4 (8.0 mg) in a mixture of the indicated solvent and TEOA (4:1, v/v; 4 mL). A Pyrex test tube with a septum (11 mL capacity) was used as the reaction vessel and a 400 W high-pressure Hg lamp with a $NaNO_2$ solution filter as the light source. Reaction time: 1 h. [b] With respect to the amount of Ru complex. Data for CO and H_2 production are shown in Table S1.

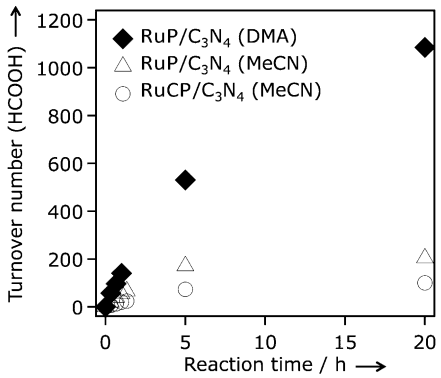

Figure 1. The turnover number of HCOOH production as a function of irradiation time using various photocatalysts. Reaction conditions: Ru complex (7.8 μmol per gram of C_3N_4)/C_3N_4 (8.0 mg) in a mixture of the indicated solvent and TEOA (4:1, v/v; 4 mL). A Pyrex test tube with a septum (11 mL capacity) was used as the reaction vessel and a 400 W high-pressure Hg lamp with a $NaNO_2$ solution filter as the light source.

Thus, the activity of a Ru complex/C_3N_4 mixture in CO_2 reduction depended on the Ru complex (Table 1, entries 1–4). Among the Ru complexes tested, RuP was the strongest promoter of CO_2 reduction. Electrochemical analyses (Figure S2) indicated that the first reduction potentials of RuP and RuH were very similar (ca. −1.4 V vs. $Ag/AgNO_3$), but more positive than those of RuCP and RuMe (ca. −1.5 V). The conduction-band minimum of the C_3N_4 material used in this study was located at −1.65 V (vs. $Ag/AgNO_3$).[13] Thus, the conduction-band electrons in C_3N_4 are able to move to the attached Ru complexes. The relatively poor performance of RuCP and RuMe can be explained in terms of the small potential difference between the two components of the hybrid material.

In addition to the larger potential difference between the conduction band of C_3N_4 and the reduction potential of RuP, the immobilization of a Ru complex onto the C_3N_4 surface should have a positive impact on electron transfer, as revealed by FT-IR spectroscopy (Figure S1). RuH, which does not possess any anchoring ligands, gave a relatively poor performance among the four Ru complexes tested, even though the first reduction potential of the complex lies at a relatively positive potential, and a relatively large CO_2 reduction current was observed at −1.65 V (Figure S2). RuMe, with a more negative reduction potential and no anchoring group, exhibited little activity for CO_2 reduction. Therefore, the reduction potential is crucial for efficient electron injection from C_3N_4 into the Ru complex, and the anchoring groups are essential for the direct coupling of the two units.

The results of the photocatalytic reactions with different Ru catalysts led to a rational strategy for the design of more efficient photocatalysts based on C_3N_4. This enabled a two- to three-fold improvement in the performance of the Ru complex/C_3N_4 system (Table 1 and Figure 1) compared to the system featuring RuCP as the catalytic unit.[13a] The vital role of the Ru complex in promoting CO_2 reduction also suggests that the performance is influenced by the reaction environment because CO_2 reduction on a metal complex proceeds by a multi-step mechanism, including the substitution of ligands by solvent molecules.[6b,24] To realize the full potential of the RuP/C_3N_4 photocatalyst, the effect of the solvent on the photocatalytic performance was investigated because the influence of the solvent on such metal complex/semiconductor hybrid systems had not been examined before.

As expected, the photocatalytic performance of RuP/C_3N_4 in the production of formic acid depended strongly on the solvent employed. As shown in Table 1 (entries 4–7), the best result was obtained when the reaction was carried out using DMA. Ishida et al. recently reported that DMA is also a useful solvent for photochemical CO_2 reductions in homogeneous systems.[3b] To elucidate how the solvent affects the activity in HCOOH production, photocatalytic H_2 evolution reactions were conducted with C_3N_4 modified with Pt nanoparticles (3 wt%) instead of RuP under argon atmosphere. Here, the photoexcited electrons in the conduction band moved to the loaded Pt, thereby reducing H^+ into H_2, while the valence-band holes were consumed by the oxidation of TEOA.[19] As listed in Table S2, a similar level of H_2 evolution activity was observed in all cases, except for the DMA/TEOA system. Even though the ability of TEOA to donate an electron decreased in the presence of H_2O,[25] H_2 evolution in the H_2O/TEOA system was identical to that achieved using other solvents (e.g., MeCN and MeOH). For the DMA/TEOA system, which exhibited an exceptionally low H_2 evolution activity, the addition of H_2O to the system increased the activity so that it reached the same level as for the other systems. These results indicate that the low level of H_2 evolution in the DMA/TEOA system is due to proton reduction, and that oxidation of TEOA by the valence-band holes in C_3N_4 is efficient independent of the solvent used. Therefore, the solvent used for CO_2 reduction exerts an effect on the CO_2 reduction step that occurs on RuP rather than on the oxidation process.

With these refinements, a TON of greater than 1000 (20 h) was achieved using the RuP/C_3N_4 photocatalyst under visible-light irradiation with an AQY of 5.7% at 400 nm (Figure 1). These numbers represent the greatest TON and AQY values that have been reported for visible-light-driven heterogeneous photocatalytic CO_2 reduction systems to date. The high selectivity for HCOOH production (ca. 80%) was also

maintained even after 20 hours of reaction (HCOOH: 67.7 μmol, CO: 17.7 μmol, H_2: 0.9 μmol). Very recently, Wang et al. also reported that carbon nitride was capable of reducing CO_2 into CO selectively with an AQY of approximately 0.9% at 420 nm when coupled to a cobalt-containing zeolitic imidazolate framework as a cocatalyst.[16b]

In summary, a Ru catalyst with maximized electron transfer efficiency from C_3N_4 was designed. Using a suitable reaction environment for the complex, but efficient photocatalytic conversion of CO_2 into HCOOH was achieved with a Ru complex/C_3N_4 hybrid material, which gave high TON (>1000) and AQY (5.7% at 400 nm) values. The overall performance of this hybrid material is thus superior to that of all heterogeneous photocatalysts used under visible-light irradiation to date. Thus, the present study clearly demonstrates the potential of heterogeneous photocatalysts that are based on carbon nitride for CO_2 reduction using visible light. An increasing number of reports describe new carbon nitride structures,[26] which suggests that the performance of this CO_2 reduction process may be improved by applying a more suitable carbon nitride material. This possibility is currently under investigation.

Received: November 18, 2014
Published online: January 7, 2015

Keywords: artificial photosynthesis · carbon dioxide fixation · carbon nitride · heterogeneous photocatalysis · semiconductors

[1] N. Armaroli, V. Balzani, *Angew. Chem. Int. Ed.* **2006**, *46*, 52 – 66; *Angew. Chem.* **2006**, *119*, 52 – 67.
[2] J. Hawecker, J. M. Lehn, R. Ziessel, *J. Chem. Soc. Chem. Commun.* **1983**, 536 – 538.
[3] a) J. M. Lehn, R. Ziessel, *J. Organomet. Chem.* **1990**, *382*, 157 – 173; b) Y. Kuramochi, M. Kamiya, H. Ishida, *Inorg. Chem.* **2014**, *53*, 3326 – 3332.
[4] K. Koike, H. Hori, M. Ishizuka, J. R. Westwell, K. Takeuchi, T. Ibusuki, K. Enjouji, H. Konno, K. Sakamoto, O. Ishitani, *Organometallics* **1997**, *16*, 5724 – 5729.
[5] H. Takeda, K. Koike, H. Inoue, O. Ishitani, *J. Am. Chem. Soc.* **2008**, *130*, 2023 – 2031.
[6] a) B. Gholamkhass, H. Mametsuka, K. Koike, T. Tanabe, M. Furue, O. Ishitani, *Inorg. Chem.* **2005**, *44*, 2326 – 2336; b) Y. Tamaki, T. Morimoto, K. Koike, O. Ishitani, *Proc. Natl. Acad. Sci. USA* **2012**, *109*, 15673 – 15678.
[7] Y. Kohno, T. Tanaka, T. Funabiki, S. Yoshida, *Chem. Lett.* **1997**, 993 – 994.
[8] K. Iizuka, T. Wato, Y. Miseki, K. Saito, A. Kudo, *J. Am. Chem. Soc.* **2011**, *133*, 20863 – 20868.
[9] T. Yui, A. Kan, C. Saitoh, K. Koike, T. Ibusuki, O. Ishitani, *ACS Appl. Mater. Interfaces* **2011**, *3*, 2594 – 2600.
[10] K. Teramura, S. Iguchi, Y. Mizuno, T. Shishido, T. Tanaka, *Angew. Chem. Int. Ed.* **2012**, *51*, 8008 – 8011; *Angew. Chem.* **2012**, *124*, 8132 – 8135.
[11] S. Sato, T. Morikawa, S. Saeki, T. Kajino, T. Motohiro, *Angew. Chem. Int. Ed.* **2010**, *49*, 5101 – 5105; *Angew. Chem.* **2010**, *122*, 5227 – 5231.
[12] K. Sekizawa, K. Maeda, K. Koike, K. Domen, O. Ishitani, *J. Am. Chem. Soc.* **2013**, *135*, 4596 – 4599.
[13] a) K. Maeda, K. Sekizawa, O. Ishitani, *Chem. Commun.* **2013**, *49*, 10127 – 10129; b) K. Maeda, R. Kuriki, X. Zhang, X. Wang, O. Ishitani, *J. Mater. Chem. A* **2014**, *2*, 15146 – 15151.
[14] J. Hong, W. Zhang, Y. Wang, T. Zhou, R. Xu, *ChemCatChem* **2014**, *6*, 2315 – 2321.
[15] J. Lin, Z. Pan, X. Wang, *ACS Sustainable Chem. Eng.* **2014**, *2*, 353 – 358.
[16] a) S. Wang, W. Yao, J. Lin, Z. Ding, X. Wang, *Angew. Chem. Int. Ed.* **2014**, *53*, 1034 – 1038; *Angew. Chem.* **2014**, *126*, 1052 – 1056; b) S. Wang, J. Lin, X. Wang, *Phys. Chem. Chem. Phys.* **2014**, *16*, 14656 – 14660.
[17] a) E. Casado-Rivera, D. J. Volpe, L. Alden, C. Lind, C. Downie, T. Vázquez-Alvarez, A. C. D. Angelo, F. J. DiSalvo, H. D. Abruña, *J. Am. Chem. Soc.* **2004**, *126*, 4043 – 4049; b) J. F. Hull, Y. Himeda, W.-H. Wang, B. Hashiguchi, R. Periana, D. J. Szalda, J. T. Muckerman, E. Fujita, *Nat. Chem.* **2012**, *4*, 383 – 388.
[18] a) Y. Wang, X. Wang, M. Antonietti, *Angew. Chem. Int. Ed.* **2012**, *51*, 68 – 89; *Angew. Chem.* **2012**, *124*, 70 – 92; b) X. Wang, S. Blechert, M. Antonietti, *ACS Catal.* **2012**, *2*, 1596 – 1606.
[19] X. Wang, K. Maeda, A. Thomas, K. Takanabe, G. Xin, J. M. Carlsson, K. Domen, M. Antonietti, *Nat. Mater.* **2009**, *8*, 76 – 80.
[20] X. Wang, X. Chen, A. Thomas, X. Fu, M. Antonietti, *Adv. Mater.* **2009**, *21*, 1609 – 1612.
[21] F. Su, S. C. Mathew, G. Lipner, X. Fu, M. Antonietti, S. Biechert, X. Wang, *J. Am. Chem. Soc.* **2010**, *132*, 16299 – 16301.
[22] Y. Shiraishi, S. Kanazawa, Y. Sugano, D. Tsukamoto, H. Sakamoto, S. Ichikawa, T. Hirai, *ACS Catal.* **2014**, *4*, 774 – 780.
[23] a) T. Yano, H. Matsui, T. Koike, H. Ishiguro, H. Fujihara, M. Yoshihara, T. Maeshima, *Chem. Commun.* **1997**, *12*, 1129 – 1130; b) T. Kimura, K. Kamata, N. Mizuno, *Angew. Chem. Int. Ed.* **2012**, *51*, 6700 – 6703; *Angew. Chem.* **2012**, *124*, 6804 – 6807; c) K. Sasano, J. Takaya, N. Iwasawa, *J. Am. Chem. Soc.* **2013**, *135*, 10954 – 10957.
[24] T. Morimoto, T. Nakajima, S. Sawa, R. Nakanishi, D. Imori, O. Ishitani, *J. Am. Chem. Soc.* **2013**, *135*, 16825 – 16828.
[25] H. Ishida, T. Terada, K. Tanaka, T. Tanaka, *Inorg. Chem.* **1990**, *29*, 905 – 911.
[26] G. Dong, Y. Zhang, Q. Pan, J. Qiu, *J. Photochem. Photobiol. C* **2014**, *20*, 33 – 50.

